Myeloid cell dynamics correlate with clinical outcomes of severe coronavirus disease 2019

Tomohiro Takano
National Institute of Infectious Diseases
Takayuki Matsumura (matt@niid.go.jp)
National Institute of Infectious Diseases https://orcid.org/0000-0003-1760-3484
Yu Adachi
National Institute of Infectious Diseases
Kazutaka Terahara
National Institute of Infectious Diseases
Saya Moriyama
National Institute of Infectious Diseases
Taishi Onodera
National Institute of Infectious Diseases
Ayae Nishiyama
National Institute of Infectious Diseases
Ai Kawana-Tachikawa
National Institute of Infectious Diseases
Shoji Miki
National Institute of Infectious Diseases
Kaori Hosoya-Nakayama
National Institute of Infectious Diseases
Midori Nakamura-Hoshi
National Institute of Infectious Diseases
Sayuri Seki
National Institute of Infectious Diseases
Natsuo Tachikawa
Yokohama Municipal Citizen's Hospital
Yukihiro Yoshimura
Yokohama Municipal Citizen's Hospital
Nobuyuki Miyata
Yokohama Municipal Citizen's Hospital
Hiroshi Horiuchi
Yokohama Municipal Citizen's Hospital
Hiroaki Sasaki

Yokohama Municipal Citizen's Hospital
Kazuhito Miyazaki
Yokohama Municipal Citizen's Hospital
Noriko Kinoshita
National Center for Global Health and Medicine
Tsutomu Sudo
National Center for Global Health and Medicine
Yutaro Akiyama
National Center for Global Health and Medicine
Rubuna Sato
National Center for Global Health and Medicine
Tadaki Suzuki
National Institute of Infectious Diseases
Tetsuro Matano
National Institute of Infectious Diseases
Yoshimasa Takahashi
National Institute of Infectious Diseases

Research Article

Keywords: COVID-19, SARS-CoV-2, human immunology, myeloid-derived suppressor cells, cytokines, chemokines

Posted Date: November 6th, 2020

DOI: https://doi.org/10.21203/rs.3.rs-100484/v3

Abstract

An expanded myeloid cell compartment is a hallmark of severe coronavirus disease 2019 (COVID-19); however, it remains unclear whether myeloid cells are beneficial or detrimental to the clinical outcome. Here, we tracked cellular dynamics of myeloid-derived suppressor cell (MDSC) subsets and examined whether any of them correlate with disease severity and prognosis by flow cytometric analysis of blood samples from COVID-19 patients. We observed that polymorphonuclear (PMN)-MDSCs, rather than other MDSC subsets, transiently expanded in severe cases but not in mild or moderate cases. Notably, this subset was selectively expanded in survivors of severe cases and diminished during recovery. Analysis of plasma cytokines/chemokines revealed that interleukin-8 increased prior to PMN-MDSC expansion in survivors and returned to basal levels during the recovery phase. In contrast, interleukin-6 and interferon-γ-induced protein 10 were abundantly induced in non-survivors, suggesting possible downstream targets for the immunosuppressive effects of the MDSC subset. Our data indicate that increased cellularity of PMN-MDSCs might be beneficial for the clinical outcome and could be useful as a possible predictor of prognosis in cases of severe COVID-19.

Introduction

In December 2019, coronavirus disease 2019 (COVID-19), caused by severe acute respiratory syndrome coronavirus 2 (SARS-CoV-2), was first reported in Wuhan, Hubei Province, China, and rapidly spread causing a global pandemic[1-5]. Although most COVID-19 patients exhibit asymptomatic or mild clinical symptoms that resemble seasonal coronavirus diseases, 19% of patients suffer from severe or critical disease with 2.3% mortality[6]. The countermeasure for the pandemic is prioritized to protect those who are at greater risk of death from COVID-19, including the elderly and those with comorbidities, such as hypertension, diabetes, and cardiac and pulmonary diseases[6,7].

Myeloid-derived suppressor cells (MDSCs) are a heterogeneous population of immature myeloid cells that are generated during a large array of pathogenic conditions from cancer to obesity and mediate immune suppression[8]. In humans, MDSCs consist of at least three groups of cells, monocytic MDSCs (M-MDSCs), polymorphonuclear MDSCs (PMN-MDSCs), and early stage MDSCs (e-MDSCs), which have been found in peripheral blood mononuclear cells (PBMCs), in addition to bone marrow and inflammatory tissues[8]. MDSCs have been reported in various infectious diseases, including bacterial, fungal, parasitic, and viral infections[9]; however, their roles in disease pathogenesis are still unclear. Notably, individuals with the aforementioned risk factors for COVID-19 are prone to sustained increased frequencies of MDSCs[8,10]. In addition, elevated levels of interleukin (IL)-6 and IL-8, well-known inducers of MDSCs[11-13], are observed in severe cases of COVID-19[14,15].

This information suggests a possible link between MDSCs and COVID-19. The expansion of MDSCs and MDSC-like cells has been repeatedly observed in severe COVID-19 patients by several research groups from different countries[16-22]. However, to gain insight into the roles of MDSCs in COVID-19, it is important

to analyze the cell subsets in association with different clinical outcomes (e.g. survivors and non-survivors). In this study, we describe the transient but prominent expansion of the PMN-MDSC subset in survivors of severe COVID-19. Along with the cytokine/chemokine levels in plasma, our data suggest the beneficial role of PMN-MDSCs, which potentially suppress excessive inflammation during recovery from severe COVID-19.

Results

Expanded PMN-MDSC subset in survivors of severe COVID-19

Three MDSC subsets (e-MDSCs, M-MDSCs, and PMN-MDSCs) in PBMCs were enumerated by flow cytometry (Supplementary Fig. S1). e-MDSCs, M-MDSCs, and PMN-MDSCs were phenotypically defined as $CD3^-CD19^-CD56^-HLA\text{-}DR^-CD11b^+CD33^+CD14^-CD15^-$, $CD3^-CD19^-CD56^-HLA\text{-}DR^-CD11b^+CD33^+CD14^+CD15^-$, and $CD3^-CD19^-CD56^-HLA\text{-}DR^-CD11b^+CD33^+CD14^-CD15^+$, respectively (Supplementary Fig. S1a)[8,23]. In agreement with a recent publication[18], we defined days 0–10 and days 11–30 following onset of the initial symptoms as early and late phases, respectively.

The frequencies of each MDSC subset among live PBMCs were tracked with time after symptom onset (Fig. 1). The results are plotted separately for the early and late phases (Fig. 2a and 2b). During the early phase, a significant reduction in e-MDSC frequencies was observed in moderate II and severe surviving cases relative to those in healthy controls (p = 0.0317, healthy vs. moderate II; p = 0.0175, healthy vs. severe surviving cases), partly similar to the results described in a recent study [22]. Therefore, the loss of e-MDSCs in peripheral blood correlates with the onset of moderate II and severe surviving cases.

Although M-MDSC and PMN-MDSC subsets remained unchanged in the early phase, the frequencies of PMN-MDSCs, rather than M-MDSCs, dramatically increased in the late phase of severe COVID-19 (Fig. 1b, 1c, 2a, and 2b), reproducing findings in recent publications[17-22]. Further extending previous findings, we found that the increase in PMN-MDSCs was transient, and the frequencies of PMN-MDSCs returned to basal levels during the recovery phase before discharge (Fig. 1c). Together, we conclude that the PMN-MDSC subset emerges in the peripheral blood stream in correlation with disease severity and declines by the time of discharge.

Subdivision of severe cases into survivors and non-survivors gives us important indications as to how the increased MDSC subset contributes to the clinical outcome and whether this subset is beneficial or detrimental to the prognosis. Notably, a selective increase of the PMN-MDSC subset, rather than the M-MDSC subset, in survivors of severe COVID-19 was observed, whereas the PMN-MDSC subset remained unchanged in non-survivors even in the late phase of severe COVID-19 (Fig. 1b, 1c, 2a, and 2b). The average time points for cellular analysis in both groups were not significantly different (survivor: day 19 ± 5, non-survivors: day 16 ± 4, mean ± SD, p = 0.35, two-tailed Student's t-test). Therefore, defective expansion of the PMN-MDSC subset in non-survivors is unlikely, owing to the analysis time differences.

Association between MDSC subsets and plasma IL-6 and IL-8 levels

To gain insight into the cytokines/chemokines that affect MDSC dynamics, we subsequently analyzed plasma levels of cytokines and chemokines, including IL-1β, IL-2, IL-4, IL-5, IL-6, IL-8, IL-10, IL-12 p70, IL-17F, granulocyte colony-stimulating factor (G-CSF), granulocyte-macrophage colony-stimulating factor (GM-CSF), interferon (IFN)-α, IFN-γ, IFN-γ-induced protein 10 (IP-10), monocyte chemotactic protein 1 (MCP-1), monokine induced by IFN-γ (MIG), macrophage inflammatory protein (MIP)-1α, and tumor necrosis factor (TNF)-α, in all donors (Fig. 3, Supplementary Fig. S2, and S3). Most cytokines/chemokines, except IL-6, IL-8, and IP-10, were not significantly elevated in cohorts of this study. As IL-6 and IL-8 are key regulators of M-MDSCs and PMN-MDSCs, respectively[11-13], we first focused on the correlation between these cytokines/chemokines and the cellularity of MDSC subsets. In the study cohorts, a significant change was observed in plasma IL-6 in severe fatal cases ($p = 0.0348$, healthy vs. severe fatal case [early phase]; $p = 0.0234$, mild case vs. severe fatal case [early phase]) in line with previous studies in which IL-6 levels tended to be higher in severe cases (Fig. 3a)[14,15,24,25]. We also observed a significant and selective increase in IL-8 levels in the early and late phases of severe cases ($p = 0.0004$, healthy vs. severe surviving case [early phase]; $p = 0.0002$, mild vs. severe surviving case [early phase]; $p = 0.0014$, moderate I vs. severe surviving case [early phase]; $p = 0.0001$, moderate II vs. severe surviving case [early phase]; $p = 0.0250$, severe surviving case vs. severe fatal case [early phase]; $p = 0.0388$, moderate I vs. severe surviving case [late phase]; $p = 0.0396$, moderate II vs. severe surviving case [late phase]; Fig. 3a and 3b)[14,15]. Notably, IL-8 elevation in the early phase was a specific event in survivors; non-survivors failed to produce as much IL-8 as the survivors (Fig. 3a).

The correlation between IL-6/IL-8 levels and each MDSC subset was subsequently examined. Plasma IL-6 levels were negatively correlated with the e-MDSC subset in this cohort (Fig. 4a), suggesting the possible involvement of IL-6 in the reduction of the e-MDSC subset. Additionally, plasma IL-6 levels were positively correlated with the M-MDSC subset (Fig. 4a). These results are consistent with the previous idea that IL-6 is a key inducer of the M-MDSC subset[11,12].

We observed a specific increase in IL-8 levels in the early phase and PMN-MDSC subset in the late phase from survivors of severe cases. These results imply a link between IL-8 and PMN-MDSC induction. In agreement with this, we observed a positive correlation between IL-8 levels and the frequencies of PMN-MDSCs, whereas this correlation was not found for IL-6 (Fig. 4a and 4b). Given the chemoattractant activity of IL-8 in the PMN-MDSC subset[13], PMN-MDSCs might be recruited into peripheral blood by IL-8 following the onset of severe COVID-19.

Association between MDSC subsets and plasma IP-10 levels

Consistent with recent reports[25,26], plasma levels of the interferon-γ-inducible chemokine IP-10 were elevated in the early phase of severe fatal cases (Fig. 3a). Similar to IL-6, this chemokine was elevated in non-survivors of severe cases (Fig. 3a). The negative correlation between IP-10 and the e-MDSC subset suggests possible involvement of this chemokine in e-MDSC reduction, in addition to IL-6 (Fig. 4a and

4c). Since IL-6 and IP-10 were abundantly induced in non-survivors (Fig. 3a and 3b), their related cells might be possible targets for the immunosuppressive effects of the PMN-MDSC subset.

Discussion

MDSCs are heterogeneous myeloid cell subsets that expand proportionally to the severity of inflammatory diseases. They are equipped with several immunosuppressive molecules; however, whether they are beneficial or detrimental to the clinical outcomes of cancer, obesity, and chronic infectious diseases remains unclear[8,9]. In agreement with this, several groups have recently reported the expansion of MDSC subsets in severe COVID-19 patients[16-22]; however, the link between MDSC subsets and clinical outcome remains to be addressed, owing to limitations in experimental design. By separately analyzing survivors and non-survivors of severe COVID-19, we revealed the expansion of the PMN-MDSC subset as a survival-specific event that is associated with recovery from the disease. Thus, our data favor a beneficial role of the PMN-MDSC subset, contributing to recovery from severe COVID-19.

Upon COVID-19 onset, the levels of the e-MDSC subset declined more substantially in moderate II and severe surviving cases than in the healthy individuals, partly consistent with results of a recent study[22]. Analysis of plasma cytokine/chemokine levels also revealed a negative correlation between e-MDSC frequencies and IL-6/IP-10 levels. The mechanism by which these factors regulate the cellularity of the e-MDSC subset remains to be elucidated in future studies. Likewise, the roles of the e-MDSC subset in COVID-19 are unknown; however, the suppression of this subset could serve as an immunological indicator of the onset of moderate II and severe surviving cases.

In patients with solid cancer, T-cell-suppressive activity is higher in PMN-MDSCs than in e-MDSCs and M-MDSCs[27]. Here, we found transient expansion of PMN-MDSCs, rather than e-MDSCs or M-MDSCs, in survivors of severe COVID-19. Perhaps transient and more effective immunosuppression by PMN-MDSCs is necessary for host survival in severe COVID-19. Alternatively, as claimed by other groups, the expansion of M-MDSCs could contribute to the immune imbalance described in COVID-19, possibly favoring disease progression[21]. Thus, the balance between PMN-MDSC and M-MDSC subsets might be crucial for regulating disease severity and could be associated with prognosis. Furthermore, we previously identified PMN-MDSC-like cells, known as IFN-γ-producing immature myeloid cells, which are key cellular components that confer protection against severe bacterial infection[28-30]. Thus, it is intriguing to speculate that additional PMN-MDSC-like cells might exist that promote recovery from severe COVID-19.

MDSCs are generally considered to play a harmful role in cancer and several infectious diseases[8,9], whereas they have a beneficial role not only in generating tolerance in autoimmune diseases and allograft transplantation but also in providing protection against sepsis[31-33]. During severe COVID-19, neutralizing antibody responses arise slower than they do against influenza viruses, become detectable after a >1-week incubation period, and peak at 3–4 weeks following symptom onset[34]. Therefore, the period prior to the induction of acquired immunity might be a key decisive point for the clinical outcome

of severe cases in which the control of viral replication without hyperinflammation is needed. Along the same line, it has been shown that the anti-inflammatory drugs dexamethasone and anti-IL-6 receptor monoclonal antibody reduce the mortality rate of severe COVID-19 cases[35-38]. We speculate that the emergence of the PMN-MDSC subset prolongs survival by suppressing excessive inflammation until acquired immunity is introduced. In agreement with the hypothesis that MDSCs can inhibit/reduce the severe lung inflammation/sepsis associated with COVID-19[39], we propose that the expansion of the PMN-MDSC subset might be beneficial for the clinical outcome and could be useful as a possible predictor of prognosis in cases of severe COVID-19.

Methods

Ethics approval and consent to participate

This study protocol was approved by the National Institute of Infectious Diseases Ethic Review Board for Human Subjects (Permit number: 1107 and 1111). All participants provided written informed consent in accordance with the Declaration of Helsinki.

Human subjects

This study enrolled 40 patients with mild (n = 12), moderate I (n = 7), moderate II (n = 8), and severe (n = 13) COVID-19 at two hospitals in Japan (Yokohama Municipal Citizen's Hospital and Center Hospital of the National Center for Global Health and Medicine), as well as seven healthy donors. The severity of symptoms was stratified according to the third edition of the medical guidelines of COVID-19 provided by the Japanese Ministry of Health, Labor and Welfare[40]. Mild cases were defined as having no pneumonia and no, or limited, clinical symptoms. Moderate I and moderate II cases were defined as the presence of pneumonia without and with the need for supplemental oxygen ($93\% < SpO_2 < 96\%$, moderate I; $SpO_2 \leq 93\%$, moderate II), respectively. Severe cases were defined as having pneumonia and respiratory distress requiring ICU admission or ventilator use. Clinical characteristics of patients and time points of blood sampling are provided in Supplementary Table S1.

Preparation of PBMCs and plasma

Blood samples were collected from the COVID-19 patients and healthy donors using a BD Vacutainer® CPTTM Tube (BD Biosciences, Franklin Lakes, NJ) and centrifuged for 20 min at 1500–1800 g at 23 °C. Following centrifugation, the cells and supernatant were isolated as PBMCs and plasma, respectively. PBMCs were washed with PBS (FUJIFILM Wako Pure Chemical Corporation, Osaka, Japan), cryopreserved in CELLBANKER 1 plus (ZENOAQ RESOURCE, Fukushima, Japan), and stored at -135 °C until further analysis. Plasma was stored at -80 °C until further analysis. For analysis, the cryopreserved PBMCs were thawed with RPMI 1640 (FUJIFILM Wako Pure Chemical Corporation) containing 10% fetal bovine serum (Nichirei Biosciences, Tokyo, Japan), 2 mM glutamine (FUJIFILM Wako Pure Chemical Corporation), 50 μM 2-mercaptoethanol (Thermo Fisher Scientific, Waltham, MA), 100 U ml^{-1} penicillin

(FUJIFILM Wako Pure Chemical Corporation), and 100 μg ml^{-1} streptomycin (FUJIFILM Wako Pure Chemical Corporation).

Flow cytometry

PBS (Nacalai Tesque, Kyoto, Japan) containing 0.5% bovine serum albumin (Roche Diagnostics, Basel, Switzerland) and 5 mM EDTA (Thermo Fisher Scientific) was used as the antibody staining buffer and wash buffer. PBMCs were incubated with Human TruStain FcX (BioLegend, San Diego, CA) for 10 min at 23 °C to avoid binding of nonspecific antibodies (Fc blocking).Following washing, PBMCs were stained with CD11b-FITC (clone ICRF44; BioLegend), CD14-BV650 (clone M5E2; BD Biosciences), CD15-APC (clone W6D3; BioLegend), CD33-APC/Cyanine7 (clone P67.6; BioLegend), CD33-BV510 (clone WM53; BD Biosciences), and HLA-DR-PE/Cy7 (clone G46-6; BD Biosciences) for 20 min at 4 °C. Additionally, 7-aminoactinomycin D (Sigma-Aldrich, St Louis, MO, USA) was used simultaneously to stain dead cells. Following thorough washing, specimens were analyzed using a FACSAria III flow cytometer (BD Biosciences). Data obtained from flow cytometry were analyzed using FlowJo v10.6.1 (BD Biosciences).

Cytokine/chemokinequantification

Plasma cytokines/chemokines were measured using a cytometric bead array kit (BD Biosciences) according to the manufacturer's instructions. Data were acquired using a FACSCalibur flow cytometer (BD Biosciences) and analyzed using FCAP Array Software Version 3.0 (BD Biosciences).

Statistical analysis

Data comprising the flow cytometric frequencies of cells were compared with two-way ANOVA with post-hoc Tukey's honest significant difference test. Average time points for cellular analysis were compared between survivors and non-survivors of severe COVID-19 at the late phase by a two-tailed Student's t-test, and a p-value < 0.05 was considered significant. For plasma cytokine levels below the detection limit, the value was set to 0.01 pg ml^{-1}. Cytokine concentrations were compared with one-way ANOVA with post-hoc Tukey's honest significant difference test. Statistical significance was set at *p < 0.05, **p < 0.01, ***p < 0.001, and ****p < 0.0001. Spearman correlations between plasma cytokine concentrations and cell frequencies were identified in all specimens. Correlations with r > 0.4 or r < −0.4 and p < 0.01 were considered significant. A simple regression line was shown for a significant correlation. GraphPad Prism version 8.0 (GraphPad Software, San Diego, CA, USA) was used for all statistical analyses and graphical representations.

Data availability

All scripts used in this manuscript are available upon reasonable request.

References

1 Li, Q. *et al.* Early Transmission Dynamics in Wuhan, China, of Novel Coronavirus-Infected Pneumonia. *N. Engl. J. Med.***382**, 1199-1207, doi:10.1056/NEJMoa2001316 (2020).

2 Zhu, N. *et al.* A Novel Coronavirus from Patients with Pneumonia in China, 2019. *N. Engl. J. Med.***382**, 727-733, doi:10.1056/NEJMoa2001017 (2020).

3 Zhou, P. *et al.* A pneumonia outbreak associated with a new coronavirus of probable bat origin. *Nature***579**, 270-273, doi:10.1038/s41586-020-2012-7 (2020).

4 Wu, F. *et al.* A new coronavirus associated with human respiratory disease in China. *Nature***579**, 265-269, doi:10.1038/s41586-020-2008-3 (2020).

5 Coronaviridae Study Group of the International Committee on Taxonomy of, V. The species Severe acute respiratory syndrome-related coronavirus: classifying 2019-nCoV and naming it SARS-CoV-2. *Nat Microbiol***5**, 536-544, doi:10.1038/s41564-020-0695-z (2020).

6 Wu, Z. & McGoogan, J. M. Characteristics of and Important Lessons From the Coronavirus Disease 2019 (COVID-19) Outbreak in China: Summary of a Report of 72314 Cases From the Chinese Center for Disease Control and Prevention. *JAMA***323**, 1239-1242, doi:10.1001/jama.2020.2648 (2020).

7 Guan, W. J. *et al.* Clinical Characteristics of Coronavirus Disease 2019 in China. *N. Engl. J. Med.***382**, 1708-1720, doi:10.1056/NEJMoa2002032 (2020).

8 Veglia, F., Perego, M. & Gabrilovich, D. Myeloid-derived suppressor cells coming of age. *Nat Immunol***19**, 108-119, doi:10.1038/s41590-017-0022-x (2018).

9 Goh, C., Narayanan, S. & Hahn, Y. S. Myeloid-derived suppressor cells: the dark knight or the joker in viral infections? *Immunol Rev***255**, 210-221, doi:10.1111/imr.12084 (2013).

10 Bueno, V., Sant'Anna, O. A. & Lord, J. M. Ageing and myeloid-derived suppressor cells: possible involvement in immunosenescence and age-related disease. *Age (Dordr)***36**, 9729, doi:10.1007/s11357-014-9729-x (2014).

11 Garg, A. & Spector, S. A. HIV type 1 gp120-induced expansion of myeloid derived suppressor cells is dependent on interleukin 6 and suppresses immunity. *J Infect Dis***209**, 441-451, doi:10.1093/infdis/jit469 (2014).

12 Fang, Z. *et al.* Polarization of Monocytic Myeloid-Derived Suppressor Cells by Hepatitis B Surface Antigen Is Mediated via ERK/IL-6/STAT3 Signaling Feedback and Restrains the Activation of T Cells in Chronic Hepatitis B Virus Infection. *J Immunol***195**, 4873-4883, doi:10.4049/jimmunol.1501362 (2015).

13 Dominguez, C., McCampbell, K. K., David, J. M. & Palena, C. Neutralization of IL-8 decreases tumor PMN-MDSCs and reduces mesenchymalization of claudin-low triple-negative breast cancer. *JCI Insight***2**, e94296, doi:10.1172/jci.insight.94296 (2017).

14 Zhang, X. *et al.* Viral and host factors related to the clinical outcome of COVID-19. *Nature***583**, 437-440, doi:10.1038/s41586-020-2355-0 (2020).

15 Li, S. *et al.* Clinical and pathological investigation of patients with severe COVID-19. *JCI Insight***5**, e138070, doi:10.1172/jci.insight.138070 (2020).

16 Bordoni, V. *et al.* An inflammatory profile correlates with decreased frequency of cytotoxic cells in COVID-19. *Clin. Infect. Dis.*, ciaa577, doi:10.1093/cid/ciaa577 (2020).

17 Agrati, C. *et al.* Expansion of myeloid-derived suppressor cells in patients with severe coronavirus disease (COVID-19). *Cell Death Differ.***27**, 3196-3207, doi:10.1038/s41418-020-0572-6 (2020).

18 Schulte-Schrepping, J. *et al.* Severe COVID-19 Is Marked by a Dysregulated Myeloid Cell Compartment. *Cell***182**, 1419-1440, doi:10.1016/j.cell.2020.08.001 (2020).

19 Silvin, A. *et al.* Elevated Calprotectin and Abnormal Myeloid Cell Subsets Discriminate Severe from Mild COVID-19. *Cell***182**, 1401-1418, doi:10.1016/j.cell.2020.08.002 (2020).

20 Zhou, R. *et al.* Acute SARS-CoV-2 Infection Impairs Dendritic Cell and T Cell Responses. *Immunity***53**, 864-877, doi:10.1016/j.immuni.2020.07.026 (2020).

21 Falck-Jones, S. *et al.* Functional myeloid-derived suppressor cells expand in blood but not airways of COVID-19 patients and predict disease severity. *medRxiv*, doi:10.1101/2020.09.08.20190272 (2020).

22 Rendeiro, A. F. *et al.* Longitudinal immune profiling of mild and severe COVID-19 reveals innate and adaptive immune dysfunction and provides an early prediction tool for clinical progression. *medRxiv*, doi:10.1101/2020.09.08.20189092 (2020).

23 Bronte, V. *et al.* Recommendations for myeloid-derived suppressor cell nomenclature and characterization standards. *Nat Commun***7**, 12150, doi:10.1038/ncomms12150 (2016).

24 Young, B. E. *et al.* Viral dynamics and immune correlates of COVID-19 disease severity. *Clin. Infect. Dis.*, ciaa1280, doi:10.1093/cid/ciaa1280 (2020).

25 Chi, Y. *et al.* Serum Cytokine and Chemokine Profile in Relation to the Severity of Coronavirus Disease 2019 in China. *J Infect Dis***222**, 746-754, doi:10.1093/infdis/jiaa363 (2020).

26 Yang, Y. *et al.* Plasma IP-10 and MCP-3 levels are highly associated with disease severity and predict the progression of COVID-19. *J. Allergy Clin. Immunol.***146**, 119-127, doi:10.1016/j.jaci.2020.04.027 (2020).

27 Lang, S. *et al.* Clinical Relevance and Suppressive Capacity of Human Myeloid-Derived Suppressor Cell Subsets. *Clin. Cancer Res.***24**, 4834-4844, doi:10.1158/1078-0432.CCR-17-3726 (2018).

28 Matsumura, T. *et al.* Interferon-gamma-producing immature myeloid cells confer protection against severe invasive group A Streptococcus infections. *Nat. Commun.***3**, 678, doi:10.1038/ncomms1677 (2012).

29 Matsumura, T. *et al.* Sequential Sensing by TLR2 and Mincle Directs Immature Myeloid Cells to Protect against Invasive Group A Streptococcal Infection in Mice. *Cell Rep.***27**, 561-571, doi:10.1016/j.celrep.2019.03.056 (2019).

30 Matsumura, T. & Takahashi, Y. The role of myeloid cells in prevention and control of group A streptococcal infections. *Biosaf Health***2**, 130-134, doi:10.1016/j.bsheal.2020.05.006. (2020).

31 Ioannou, M. *et al.* Crucial role of granulocytic myeloid-derived suppressor cells in the regulation of central nervous system autoimmune disease. *J Immunol***188**, 1136-1146, doi:10.4049/jimmunol.1101816 (2012).

32 Dilek, N., Vuillefroy de Silly, R., Blancho, G. & Vanhove, B. Myeloid-derived suppressor cells: mechanisms of action and recent advances in their role in transplant tolerance. *Front Immunol***3**, 208, doi:10.3389/fimmu.2012.00208 (2012).

33 Esher, S. K., Fidel, P. L., Jr. & Noverr, M. C. Candida/Staphylococcal Polymicrobial Intra-Abdominal Infection: Pathogenesis and Perspectives for a Novel Form of Trained Innate Immunity. *J Fungi (Basel)***5**, 37, doi:10.3390/jof5020037 (2019).

34 Iyer AS *et al.* Dynamics and significance of the antibody response to SARS-CoV-2 infection. *medRxiv*, doi:10.1101/2020.07.18.20155374 (2020).

35 Horby, P. *et al.* Dexamethasone in Hospitalized Patients with Covid-19 - Preliminary Report. *N. Engl. J. Med.*, doi:10.1056/NEJMoa2021436 (2020).

36 Biran, N. *et al.* Tocilizumab among patients with COVID-19 in the intensive care unit: a multicentre observational study. *Lancet Rheumatol***2**, e603-e612, doi:10.1016/S2665-9913(20)30277-0 (2020).

37 Guaraldi, G. *et al.* Tocilizumab in patients with severe COVID-19: a retrospective cohort study. *Lancet Rheumatol***2**, e474-e484, doi:10.1016/S2665-9913(20)30173-9 (2020).

38 Xu, X. *et al.* Effective treatment of severe COVID-19 patients with tocilizumab. *Proc Natl Acad Sci U S A***117**, 10970-10975, doi:10.1073/pnas.2005615117 (2020).

39 Fidel, P. L., Jr. & Noverr, M. C. Could an Unrelated Live Attenuated Vaccine Serve as a Preventive Measure To Dampen Septic Inflammation Associated with COVID-19 Infection? *mBio***11**, e00907-00920, doi:10.1128/mBio.00907-20 (2020).

40 Ministry of Health, Labour and Welfare, Japan. COVID-19 medical guideline https://www.mhlw.go.jp/content/000668291.pdf (2020).

Declarations

Acknowledgments

We thank Michio Aiko, Rutaro Iwabuchi, Yasuko Tsunetsugu-Yokota, and Manabu Ato for technical support; and Ryoko Itami for secretarial assistance. This work was supported by the Japan Agency for Medical Research and Development (grant numbers: JP19fk0108104 and JP20fk0108104 to T. Suzuki and Y.T.).

Author contributions statement

TT, T. Matsumura, and YT conceived and designed the study, interpreted the results, and wrote the manuscript. TT and T. Matsumura conducted the experiments and performed data analysis. TT, T. Matsumura, Y. Adachi, KT, SM, TO, AN, AK-T, SM, KH-N, MN-H, and SS prepared and processed clinical samples. NT, YY, NM, HH, HS, KM, NK, T. Sudo, Y. Akiyama, and RS collected clinical samples and clinical information. NT, T. Suzuki., and T. Matano contributed to the interpretation of the results and prepared the manuscript, and all authors discussed the results and commented on the manuscript.

Competing interests statement

The authors declare no competing interests.

Figures

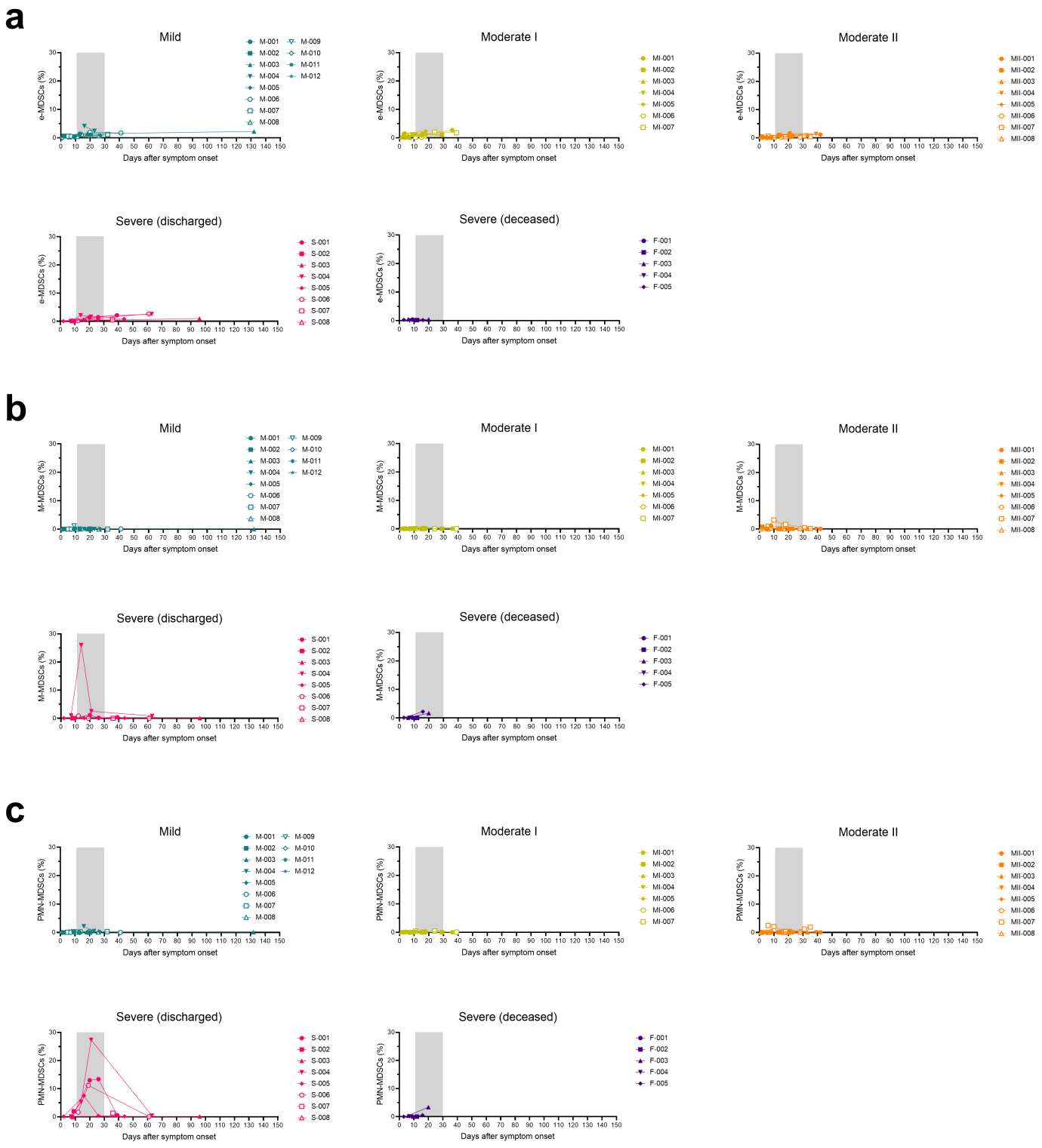

Figure 1

Longitudinal analysis of frequencies of MDSC subsets in COVID-19 patients. The frequencies of e-MDSCs (a), M-MDSCs (b), and PMN-MDSCs (c) at different time points were analyzed. Each symbol indicates individual patients described at the right of the plot. The late phase (days 11–30) is highlighted in gray.

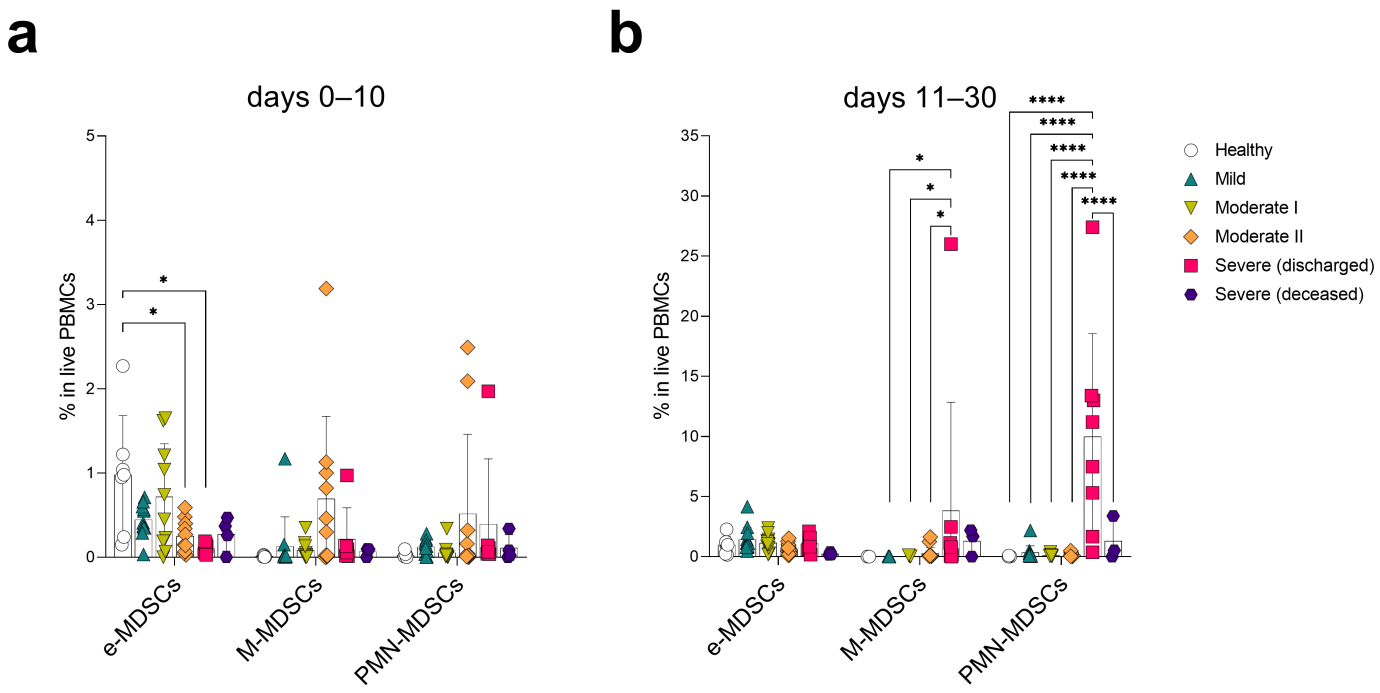

Figure 2

Analysis of the frequencies of MDSC subsets in COVID-19 patients. The frequencies of each MDSC subset were analyzed at the early phase (days 0–10; a) and the late phase (days 11–30; b). Data are represented as points indicating the data of independent samples and the mean (bar) ± SD of independent samples. Healthy donors, n = 7, n' = 7. Days 0–10, COVID-19 mild cases, n = 11, n' = 10; moderate I cases, n = 10, n' = 6; moderate II cases, n = 10, n' = 6; severe surviving cases, n = 6, n' = 6; severe fatal cases, n = 4, n' = 4. Days 11–30, COVID-19 mild cases, n = 13, n' = 8; moderate I cases, n = 12, n' = 7; moderate II cases, n = 14, n' = 8; severe surviving cases, n = 8, n' = 4, severe fatal cases, n = 3, n' = 3 (n, samples; n', individuals). Two-way ANOVA and Tukey's post-hoc test were performed for statistical analysis (*$p < 0.05$, ****$p < 0.0001$).

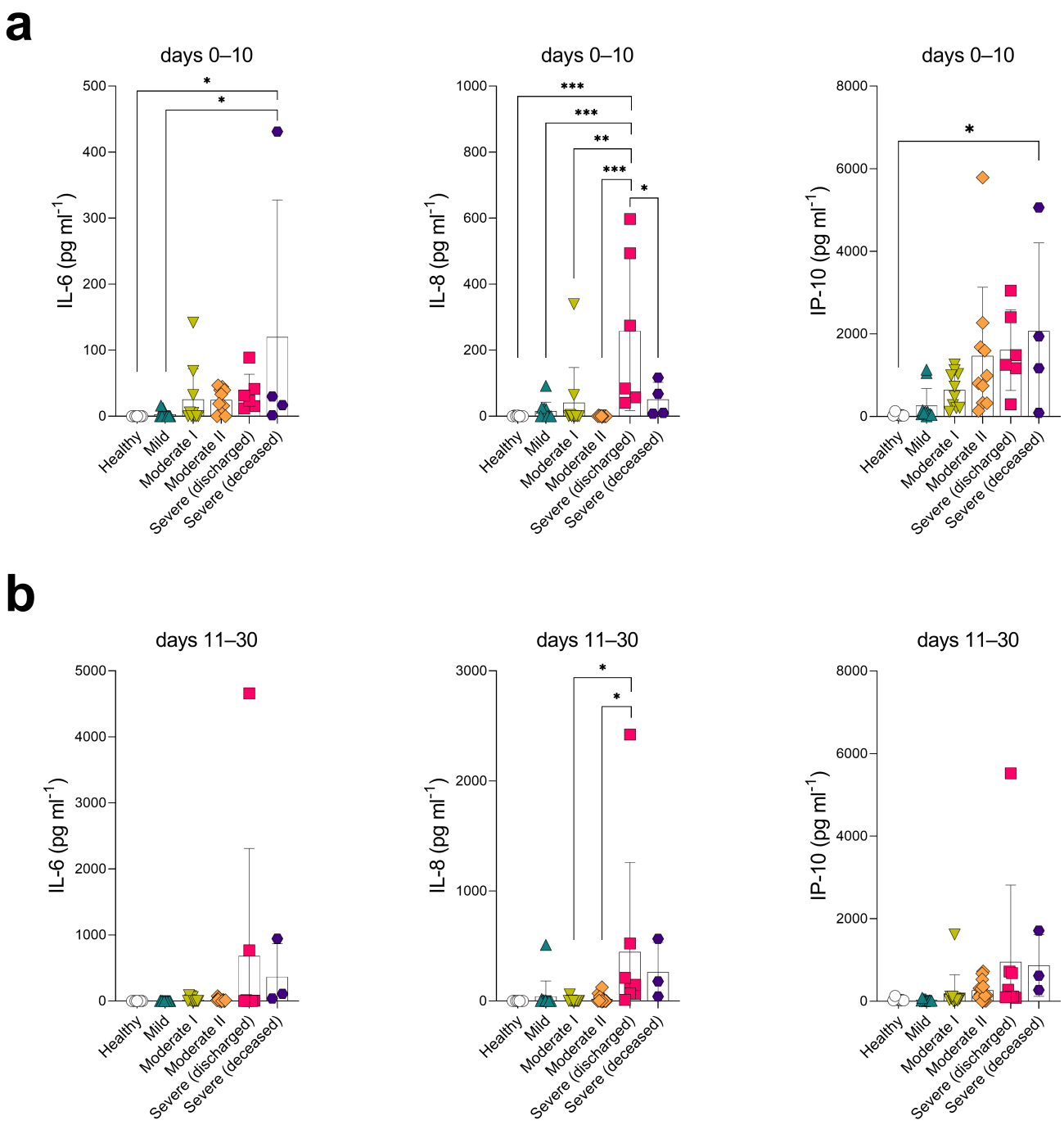

Figure 3

Analysis of plasma cytokines/chemokines in COVID-19 patients. Concentrations of plasma cytokines/chemokines (IL-6, IL-8, IP-10) were analyzed at the early phase (days 0–10; a) and the late phase (days 11–30; b). Data are shown as points indicating the data of independent samples and the mean (bar) ± SD of independent samples. Healthy donors, n = 7, n' = 7. COVID-19 mild cases, n = 11, n' = 10; moderate I cases, n = 10, n' = 6; moderate II cases, n = 10, n' = 6; severe surviving cases, n = 6, n' = 6; severe fatal cases, n = 4, n' = 4 (n, samples; n', individuals). One-way ANOVA and Tukey's post-hoc test were performed for statistical analysis (*p < 0.05, **p < 0.01, ***p < 0.001).

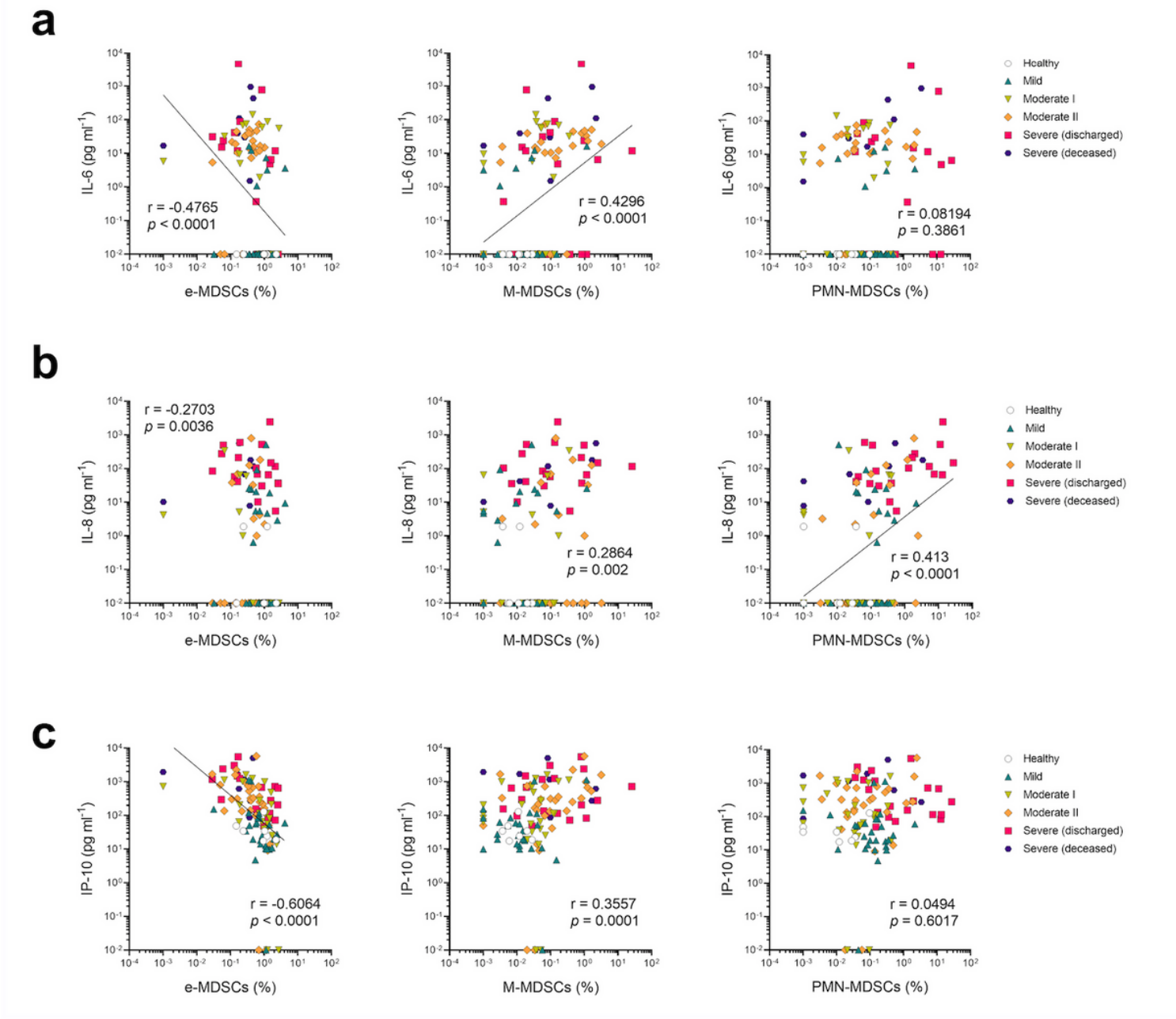

Figure 4

Associations between MDSC subsets and plasma cytokines/chemokines levels. Correlations between plasma IL-6 (a), IL-8 (b), or IP-10 (c) concentrations and frequencies of e-MDSCs, M-MDSCs, or PMN-MDSCs were analyzed. Healthy donors, n = 7, n' = 7; COVID-19 mild cases, n = 27, n' = 12; moderate I cases, n = 24, n' = 7; moderate II cases, n = 29, n' = 8; severe surviving cases, n = 20, n' = 8; severe fatal cases, n = 7, n' = 5. Spearman's rank correlation coefficients, P values, and linear regression lines are indicated in plots. Correlations with |r| > 0.4 and p < 0.01 were considered significant.

Supplementary Files

This is a list of supplementary files associated with this preprint. Click to download.

- FigureS1.TIF
- FigureS2.TIF
- FigureS3.TIF
- TableS1.pdf